

<sup>1,\*</sup>Lintao Zhang<sup>2</sup>Hongfu Qiang<sup>3</sup>Yujie Zhu<sup>4</sup>Dudou Wang<sup>5</sup>Yuxiang Liu

## The Numerical Simulation of Marangoni Problems Employing Multi-phase Parallel SPH Method



**Abstract:** - When facing microscale problems, the phenomenon of droplet movement caused by temperature gradients is usually attributed to the Marangoni effect. This study first constructed a multiphase smoothed particle fluid dynamics (SPH) system structure, integrating continuous surface force (CSF) model and multiphase model to explore the behavior of droplets under Marangoni effect. To further improve computational efficiency, this study also utilized the Open Multi Processing (OpenMP) parallel computing framework to perform parallel optimization on the SPH algorithm. Subsequently, the effectiveness of the constructed SPH framework in addressing thermal capillary phenomena was verified by simulating the Marangoni migration phenomenon of silicone oil droplets in fluorine solutions. In addition, this study also investigated the polymerization process of two droplets in microchannels under the Marangoni effect, and obtained the complete dynamic changes of droplets from motion to polymerization. During this period, we conducted a detailed analysis of the variation process of the velocity vector field, the spatial distribution of the temperature field, and the evolution characteristics of the surface tension gradient during the droplet movement process, thereby comprehensively revealing how the Marangoni effect drives the phenomenon of droplet movement and aggregation.

**Keywords:** Smoothed Particle Hydrodynamics, The Marangoni Problem, Numerical Simulation, Multi-Phase, Parallel SPH Framework

### I. INTRODUCTION

Due to the influence of temperature gradient, the gradient of surface tension drives the droplet to migrate and thus forms the flow inside the droplet, which is known as the Marangoni problem. In 1959, Young et al. [1] established the linear theoretical model of Marangoni convection problem for the first time. But only the first-order terms were calculated in the governing equation in this model. Young calculated an analytical solution (abbreviated as YGB solution) for a linear model of the droplets and bubbles' Marangoni migration process. Later, Subramanian[2], Thompson[3], Crespo[4] et al. gradually carried out nonlinear research on thermal capillaries, and modified the model of unsteady droplet migration problem.

In the field of numerical simulation, scholars have done a lot of work on special phenomena in fluid dynamics such as bubble and droplet migration. Balasubramaniam's research [5] focuses on exploring the effects of different Reynolds numbers and Marangoni numbers on the final velocity of bubble migration, revealing the motion laws of bubbles in complex flow fields through numerical simulations. Gao [6] used an axisymmetric model to simulate the thermal capillary driven motion of a single droplet under different Marangoni numbers in detail.

The author surnamed Wang [7] proposed an improved Multi Particle Fluid Dynamics (MPS) method, which is particularly suitable for studying free surface flow problems driven by thermal capillary action. The innovation of his method lies in clearly constructing surface nodes representing the boundaries of free surfaces, and incorporating Marangoni stress as a boundary condition into the simulation, achieving precise modeling through Taylor series expansion and least squares method. However, using theoretical models to solve complex problems involving non-stationary states and interactions between multiple droplets or bubbles poses certain challenges.

With the advancement of computational theory and computer technology, Computational Fluid Dynamics (CFD) has become an important means of in-depth analysis of complex fluid flow phenomena. Compared to theoretical models and experimental methods, numerical simulation can provide more dimensional and detailed flow field information. Numerical methods can be roughly divided into two categories based on discretization techniques: grid based methods and particle based methods. Grid based methods encounter significant difficulties in handling complex flows involving free surfaces, deformable boundaries, or moving interfaces due to their limitations in preset grid structures. The particle based approach, by utilizing a set of arbitrarily distributed particles,

<sup>1</sup> Xi'an Hi-Tech Institute, Xi'an 710025, China

<sup>2</sup> Xi'an Hi-Tech Institute, Xi'an 710025, China

<sup>3</sup> Xi'an Hi-Tech Institute, Xi'an 710025, China

<sup>4</sup> Xi'an Hi-Tech Institute, Xi'an 710025, China

<sup>5</sup> Xi'an Hi-Tech Institute, Xi'an 710025, China

\*Corresponding author: Lintao Zhang

Copyright © JES 2024 on-line : journal.esrgroups.org

more flexibly adapts to the simulation needs of free form surfaces or large deformation flow problems, demonstrating unique advantages.

In the realm of particle-based computational techniques, Smoothed Particle Hydrodynamics (SPH), initially conceptualized by Lucy[8] and later developed in depth by Gingold and Monaghan[9] for addressing astrophysical fluid dynamics issues, attracts more and more attention since the invention. In SPH, a set of particles are adopted to represent the flow variables and approximate the governing equations. Besides, SPH method can take into account the variation of density, thermal conductivity, viscosity and other physical property parameters in solving the problem of thermal capillarity caused by temperature change. These advantages of SPH methods make it convenient to solve the Marangoni problem of multiple droplets or bubbles. It's easy to be extended to a wider range of applications, and has great development potential. However, for Marangoni problems, there are few reports illustrating the computational mode with SPH method. SPH is a modeling method with extremely high computational requirements, which is due to the need for a large number of calculations to simulate the interaction between particles [10]. Traditional computing power is not enough to make SPH simulation run quickly, especially compared with finite element or finite volume methods. In order to obtain sufficient accuracy, Indeed, in simulations using smoothed particle hydrodynamics (SPH) or similar particle-based methods, [11]. Hardware acceleration is necessary if large cases are to be modeled. Open multiprocessing (Open MP) [12] is a set of compiler instructions and library routines that allow programming languages to take advantage of shared memory architectures. In the process of SPH simulation, the simulation calculation can be divided into serial main thread and multiple parallel slave threads, so as to improve the computational efficiency.

In this paper, the Marangoni migration computational model suitable for SPH method is first established. Then, based on the established solver the Marangoni problem of droplets are studied. In a typical scientific paper discussing multiphase flow simulations, after introducing the context and stating the importance of considering a large number of particles for accurate representation, the subsequent section would typically delve into the mathematical underpinnings that govern such systems. Here's how Section 2 might be outlined:, the SPH discretization, the CSF surface tension model, and parallel computing method. Section 3 simulates the Marangoni migration of silicone oil droplets in fluorine solution and compares it with the results of Level Set method. Furthermore simulates the polymerization problem of two droplets in the microchannel, And the evolution process of the velocity vector field, the distribution characteristics of the temperature field, and the variation law of the surface tension gradient were studied, and a summary conclusion was drawn in the fourth part.

## II. NUMERICAL METHODS

### A. Governing Equation

In this work, equations involving conservation mass, momentum and energy are considered[13], which yield:

$$\frac{D\rho}{Dt} = -\rho\nabla \cdot \mathbf{v} \tag{1}$$

$$\frac{D\mathbf{v}}{Dt} = -\frac{1}{\rho}\nabla p + \mathbf{F}^{(v)} + \mathbf{F}^{(s)} \tag{2}$$

$$\rho c_p \frac{DT}{Dt} = -p\nabla \cdot \mathbf{v} + \nabla \cdot (k\nabla T) + \Phi + Q \tag{3}$$

In Eqs (1-3),  $\frac{d}{dt}$ ,  $p$ ,  $\rho$ ,  $\mathbf{v}$ ,  $\mathbf{F}^{(v)}$ ,  $\mathbf{F}^{(s)}$  are the material derivative, pressure, density, particle velocity,

viscous term, and the surface tension term.  $c_p$  is the specific heat capacity at constant pressure; Q is the heat released from chemical reactions;  $\Phi$  is the viscous dissipation; k is the heat transfer coefficient.

To enclose the equations, the weakly compressible equation of state[14] is adopted:

$$P = P_0 \left[ \left( \frac{\rho}{\rho_0} \right)^\gamma - 1 \right] \tag{4}$$

Where  $P_0$  is the reference pressure in calculation,  $P_0 = 100\rho_0 v_{\max}^2 / \gamma$ ,  $\rho_0$  is the initial density,  $v_{\max}$  is the maximum velocity of flow field;  $\gamma$  is the constant.

*B. Multiphase SPH Equations*

In the process of droplet movement, droplet deformation may occur, and the traditional SPH method cannot obtain the kernel approximate accuracy consistent with the computational domain when the particle distribution density is inconsistent. The completely smoothed length SPH method [15], [16] corrected the calculation deviation caused by the smoothed length effect in the traditional SPH method. The smooth length is regarded as an independent coordinate variable and varies with the particle motion. In order to keep the number of adjacent particle` smoothed equations obtained by discretization based on Lagrange control equations:

$$\frac{d\rho_i}{dt} = \sum_{j=1}^N m_j \left[ \mathbf{v}_{ij} \cdot \nabla_i W_{ij} + \frac{1}{2} \left( \frac{dh_i}{dt} + \frac{dh_j}{dt} \right) \frac{\partial W_{ij}}{\partial h} \right] \tag{5}$$

$$\frac{d\mathbf{v}_i}{dt} = - \sum_{j=1}^N m_j \left( f_i \frac{P_i}{\rho_i^2} + f_j \frac{P_j}{\rho_j^2} + \Pi_{ij} \right) \nabla_i W_{ij} \tag{6}$$

The dynamic change of smooth length is:

$$\frac{dh_i}{dt} = - \frac{1}{d} h_i \frac{d\rho_i}{dt} \tag{7}$$

$f_i$  is the correction coefficient, which is expressed by the following formula:

$$f_i = \left( 1 + \frac{h_i}{d\rho_i} \sum_{j=1}^N m_j \frac{\partial W_{ij}}{\partial h_i} \right)^{-1} \tag{8}$$

$\Pi_{ij}$  is artificial viscosity, Whose expression is referred to Ref.[7].The rate of change of smooth length is correlated with the rate of change of density. In this paper, The Leapfrog method is an explicit numerical scheme commonly used in solving partial differential equations (PDEs).

In the Smoothed Particle Hydrodynamics (SPH) method, enforcing solid-wall boundary conditions can prove challenging compared to mesh-based methods due to it's Lagrange nature. In this particular research, the presence of a complex slip boundary condition at the interface between the droplet and the shell requires careful consideration.

To address this issue, the paper employs a solid-wall boundary treatment based on the virtual particle method mentioned in reference [17]. This approach ensures that fluid particles do not penetrate the solid-wall boundary, thereby avoiding numerical inaccuracies such as spurious oscillations around the boundary region.

In terms of the kernel function utilized for interpolating and spreading properties among particles, a cubic spline function is chosen for its high accuracy and smoothness. For advancing the solution in time, the Leapfrog algorithm—an explicit time integration scheme—is adopted, as detailed in reference [18]. This Leap-frog scheme allows for a stable and computationally efficient progression of the simulation through time steps while maintaining acceptable levels of accuracy and stability, particularly important in capturing the intricate dynamics at play in the system under study.

*C. CSF Surface Tension Model*

In this paper, the calculation of surface tension is approached using the Continuum Surface Force (CSF) model, [19], which describes the surface tension of the fluid as a continuous force from the boundary to the finite thickness of the interior. Morris[20] used the CSF model to deal with the surface tension for the first time in the SPH calculation. In this paper, the CSF model was partially improved in dealing with the multiphase flow problem. In this model, the body force  $\mathbf{F}_s$  is used to represent the surface tension:

$$\mathbf{F}_s = \mathbf{f}_s \delta_s \tag{9}$$

Where  $\mathbf{f}_s$  and  $\delta_s$  are the element surface force and the surface dirac function, respectively.  $\mathbf{f}_s$  can be calculated through:

$$\mathbf{f}_s = \sigma k(\mathbf{x}) \hat{\mathbf{n}} \tag{10}$$

Where,  $k(\mathbf{x})$  is the curvature of the interface position  $\mathbf{x}$ ,  $\sigma$  is the surface tension coefficient,  $\hat{\mathbf{n}}$  Is the unit normal of the interface.

The color functions defined for the different phase fluids are as follows:

$$c_i^j = \begin{cases} 1, & \text{particle } i \text{ and } j \text{ are the different phases} \\ 0, & \text{particle } i \text{ and } j \text{ are the same phases} \end{cases} \quad (11)$$

Interpolating the color function:

$$\bar{c}_i = \sum_{j=1}^N \frac{m_j}{\rho_j} c_j W_{ij} \quad (12)$$

Where,  $\bar{c}_i$  represents the color function value after particle  $i$  interpolation. Indeed, in the context of the CSF model or other numerical methods where a color function (or level set method) is used to track the interface between two phases, the normal direction at the boundary can be calculated as the gradient direction of that color function.

$$\mathbf{n} = \nabla c(\mathbf{r}) \quad (13)$$

SPH discretization on Eq.(14):

$$\mathbf{n}_i = \sum_j \frac{m_j}{\rho_j} (\bar{c}_j - \bar{c}_i) \nabla_i \cdot W_{ij} \quad (14)$$

At the same time, use the valve function  $\xi$  to eliminate the interference of particles far away from the boundary on the normal direction.

$$\hat{\mathbf{n}}_i = \begin{cases} \mathbf{n}_i / |\mathbf{n}_i|, & \text{if } |\mathbf{n}_i| > \xi \\ 0, & \text{else} \end{cases} \quad (15)$$

Where  $\xi = 0.0001 / h$ .

The interface curvature can be calculated through:

$$\kappa_i = -(\nabla \cdot \hat{\mathbf{n}})_i = \sum_j \min(N_i, N_j) \left[ \frac{m_j}{\rho_j} (\hat{\mathbf{n}}_i - \hat{\mathbf{n}}_j) \cdot \nabla_i W_{ij} \right] \quad (16)$$

#### D. Parallel Computing Optimization

In order to improve the computational efficiency of the SPH model, this study adopts the Open Multi Processor (OpenMP) parallel computing framework for optimization. This framework is based on a shared memory system design, which implements parallel execution of specified parts of a program by inserting specific instructions, retaining the structure of the original serial program and simplifying the complexity of parallel programming.

On this basis, this study constructed a multiphase thermocapillary flow simulation framework based on the SPH method, integrating multiphase flow calculation models and surface tension computer systems. By leveraging the advantages of the Open MP parallel computing framework, the SPH algorithm has been parallelized to improve computational efficiency.

Here, we implement a Splitting Cell-Linked List (CLL) technique to optimize the computational efficiency of the SPH model. This method partitions the computational domain into uniformly sized cells to shrink the search space for neighboring particles [21]. The dimension of each cell is set to be equivalent to the cutoff radius of the kernel function, denoted as 'r'. Subsequently, these cells are further split into nine smaller blocks, allowing us to allocate all cells into these blocks strategically. The neighboring particle search strategy based on CLL method is used to sort the particle data according to the grid cell index and create an array to store the indexes of the first and last particles in the grid cell in memory to ensure the sequential access to the particle data in memory and improve the access speed.

At the same time, the computing efficiency is improved by optimizing and balancing the computing load of each node through traversal mode in the computing process.

### III. NUMERICAL SIMULATION

#### A. Single Droplet Thermocapillary Migration Problem

In a flow field containing droplets, when there is a temperature gradient in the flow field, the surface tension of the droplets changes with temperature. This non-uniform surface tension will cause an unbalanced force around the droplet in the flow field, which will cause the flow field flow at the droplet interface. Cells are formed in the

inner flow field of the droplet under the action of thermocapillary, and the outer flow field presents a flow around the droplet. This movement of liquid droplets from low temperature to high temperature is called thermocapillary (Marangoni) migration[22].

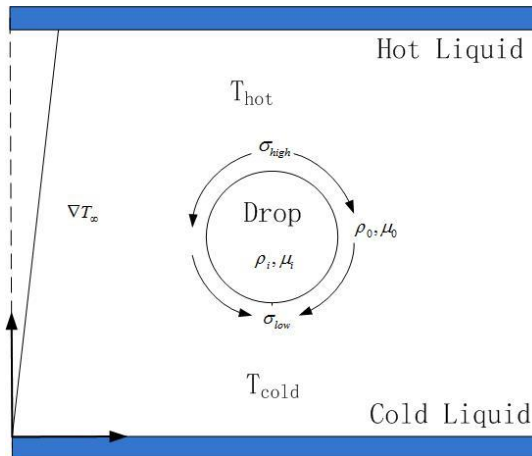


Figure 1: Thermocapillary Migration Motion of Droplets

The SPH method was used to calculate the thermocapillary migration motion of No. 5 silicone oil droplets in FC-75 fluorine solution. setting model is shown in the Figure 1, and the total number of particles in the model is 44,000. The initial temperature gradient in the Y direction is, and the calculation is performed using No. 5 silicone oil. silicone oil in the Table 1:

Table 1: Physical Properties of Silicone Oil

$T / K$	$\rho / \text{kg} \cdot \text{m}^{-3}$	$\lambda / \text{W} \cdot \text{m}^{-1} \cdot \text{K}^{-1}$	$\mu / 10^{-3} \text{N} \cdot \text{s} \cdot \text{m}^{-2}$	$\sigma / \text{N} \cdot \text{m}^{-1} \cdot \text{K}^{-1}$
293.0	918.8	0.1116	4.68	$-7.8 \times 10^{-5}$
303.0	915	0.1100	3.74	
313.0	890.8	0.1087	3.41	
323.0	887	0.1083	2.86	
333.0	878	0.1069	2.52	

The physical properties of the silicone oil at each temperature can be obtained by using the interpolation calculation method, and the calculation time step  $\Delta t = 2 \times 10^{-4} \text{ s}$ .

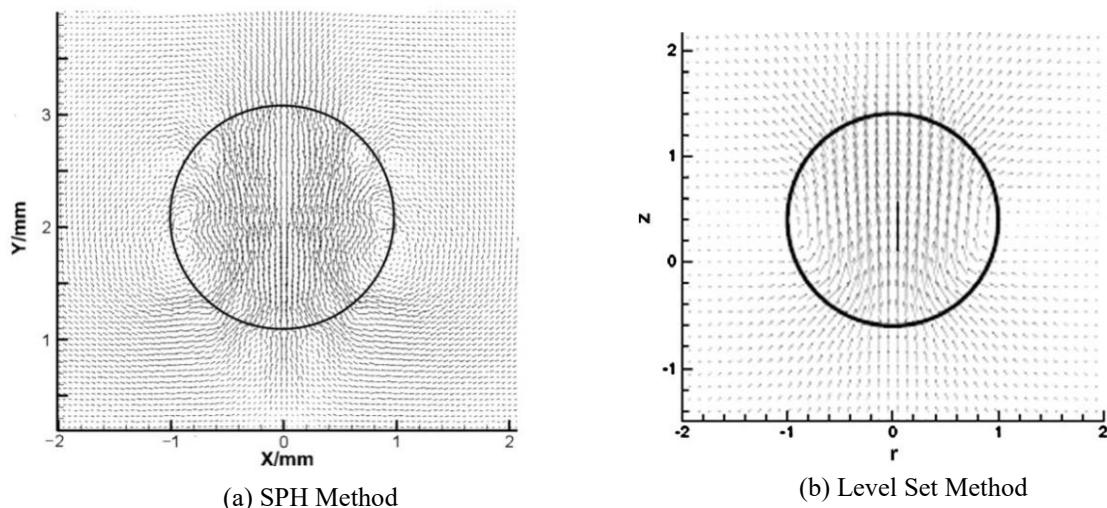


Figure 2: T=4s, Droplet Thermocapillary Migration Velocity Distribution

Figure 2 is the distribution of velocity calculated using the SPH method and using the Level-set method [6] when T=4s.

In the simulation results of the SPH method shown in the left figure, we can observe that due to the influence of thermal capillary effect, particles migrate in a positive direction along the Y-axis in the droplet centerline area, thus shaping an upward streamline; Subsequently, the flow field diffuses along the periphery of the droplet and descends on both sides of the droplet, forming small vortices on each side. This phenomenon is shown similarly in the results calculated using the level set method in the figure on the right. The simulation conclusions of the two on the internal flow field structure of droplets are basically consistent.

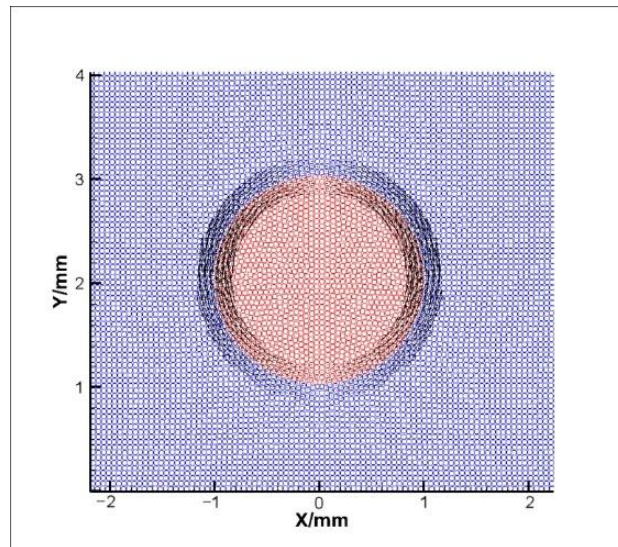


Figure 3: Surface Tension Gradient Distribution of Droplet Thermocapillary Migration Motion

The temperature difference between the front and rear ends of the droplet causes the formation of a surface tension gradient. From Image 3 (which should refer to the specific image number, possibly a typo, should be Figure 3 or other), it can be observed that the surface tension gradient exhibits a symmetrical distribution feature. This means that in the X-axis direction, the surface tension differences generated by the surface tension gradient are balanced with each other, and will not cause net movement of droplets on the X-axis. However, it is precisely this surface tension gradient that generates a forward net driving force in the Y-axis direction perpendicular to the X-axis, driving the droplets to move forward along the Y-axis direction. In the end, this driving force became the main source of driving the movement of droplets.

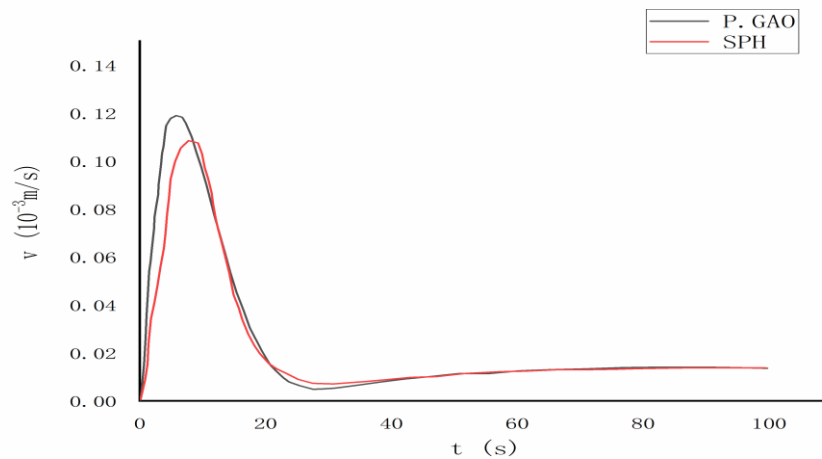


Figure 4: Droplet Migration Velocity Graph

As illustrated in Figure 4, the change of droplet migration velocity over time. At the beginning time, due to the large temperature difference, the surface tension difference between the front and rear droplet is large, and the surface tension drives the droplet movement speed to increase gradually. When  $t=1s$ , the droplet migration velocity reaches the maximum velocity. Afterwards, due to viscous dissipation and the temperature difference decrease, the force of droplet migration gradually weakened, and the droplet migration velocity gradually decreased. Compared with Gao's results, the time to reach the peak of migration velocity is relatively lag. The maximum migration velocity is slightly smaller than the calculation results in reference [6].

*B. Double Droplet Polymerization in Microchannels*

When studying the effect of thermal capillary action on the behavior of double droplets in a wet wall environment, we conducted an experiment in a microchannel scene with a width of 0.05 cm and a length of 0.11 cm, as shown in Figure 5. Two identical droplets with a radius of 0.01 centimeters were placed in this environment, and the oil phase was used as a continuous flow medium. The solid walls on both sides of the microchannel have applied adiabatic boundary conditions to ensure that heat is not transferred to the outside world. At the beginning

of the experiment, the droplets have been fully wetted on the solid wall to form a stable contact layer, which is constrained by surface tension and maintains a stable shape. That is, the droplets moderately expand along the wall due to wall adhesion. In the process of introducing external fluid drive, we focused on considering the influence of temperature changes on viscosity and surface tension. Through numerical simulation, we thoroughly analyzed the interaction and polymerization process of two droplets under temperature induced thermal capillary effect under these conditions. This series of calculations aims to reveal how temperature gradients affect the velocity, aggregation time, and final morphology of droplets.

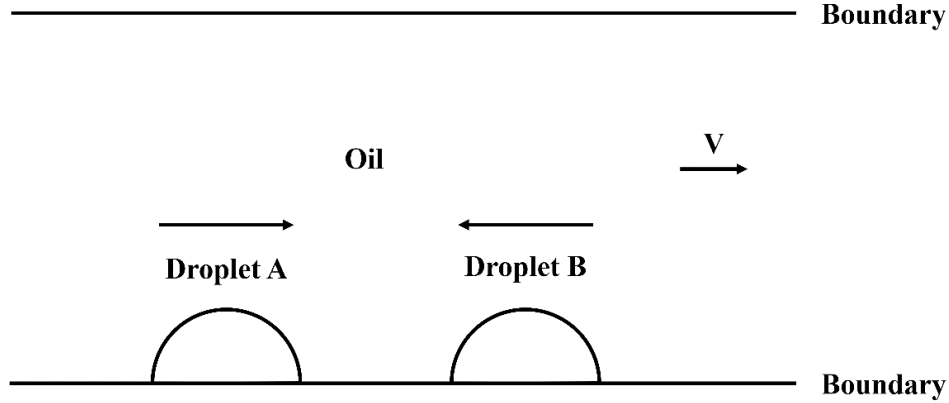


Figure 5: Polymerization Process of Two Droplets in Microchannel

The initial parameters of the model is as shown in Table 2:

Table 2: Physical Parameters of the Simulation Model

$v_{oil}$	$v_{A,B}$	$T_A$	$T_B$	$T_{oil}$	$\rho_{water}$	$\rho_{oil}$
$400\mu m / s$	$400\mu m / s$	333K	293K	293K	$1000kg / m^3$	$890kg / m^3$

In the calculation process, the time stepping method adopts the Leap-frog form, the time step is  $\Delta t = 1.0 \times 10^{-4} s$ . The calculation is carried out for a total of 16000 time steps. The viscosity and thermal conductivity of the water and oil phases vary with temperature. As a result, the surface tension of the droplet changes with temperature, resulting in thermocapillary action.

The viscosity of the water phase varies with temperature as follows:  
 $\mu_{water} = \mu_{water0} / (1 + 0.0337t + 0.000221t^2)$ ,  $\mu_{water0} = 1.792 \times 10^{-3} Pa \cdot s$  ;

The viscosity of the oil phase varies with temperature as follows:  
 $\mu_{oil} = \mu_{oil0} / (1 + 0.0337t + 0.000221t^2)$ ,  $\mu_{oil0} = 5.92 \times 10^{-3} Pa \cdot s$  ;

The thermal conductivity of the water phase varies with temperature as follows:  
 $\lambda = -1.95626 + 0.178T - 3.95068 \times 10^{-5} T^2$ , T is the Kelvin temperature;

The contact Angle  $\theta$  is used to represent the wetting condition of the wall surface by droplet, and its relationship with temperature is as follows:  $\theta = -0.2 \times (T - 273.15) + 116$

The simulation results are as follows:

It can be seen from Figure 6 (a) that at the initial moment  $t=0$ , both droplets are in a wetted state and remain stable at the bottom of the channel. After that, the two droplets move toward each other in the oil; As shown in Figure 6(b), when  $t=0.6s$ , the two droplets begin to contact gradually. In Figure 6(c), when  $t=1.2s$ , droplet A gradually climbs along the surface of droplet B. And under the action of surface tension and hot capillarity, the two droplets gradually converge. Under the influence of surface tension, the kinetic energy and surface energy of the droplet transform each other, and finally, under the action of viscosity, the kinetic energy is gradually consumed. In Figure 6(d), when  $t=1.6s$ , the new droplets formed by polymerization gradually stabilized at the bottom of the droplet in an elliptical shape.

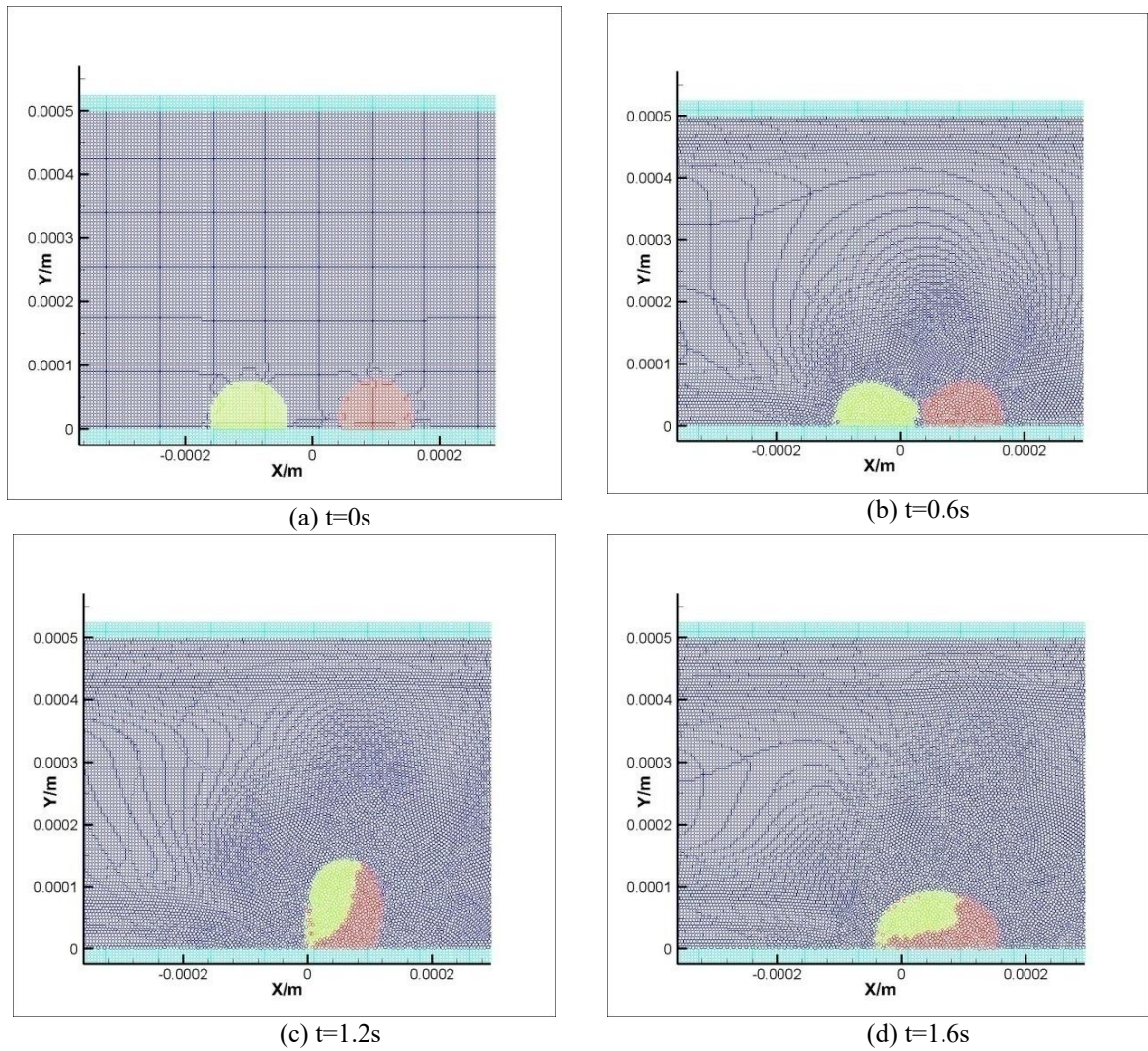


Figure 6: Particle Distribution Diagram of Double Droplet Microchannel Polymerization Problem

Without considering the thermal capillary effect, we also used the SPH method to simulate and compare similar situations. Figure 7 shows the convergence of the dual droplet motion trajectory without thermal capillary effect. Clearly, due to the neglect of the Marangoni effect, the velocity of droplet A moving to the right is significantly increased, leading to an earlier intersection time with droplet B from  $t=0.6s$  to  $t=0.39s$ . In addition, when the thermal capillary phenomenon is not calculated, the wetting angle of the droplets is relatively small. Although the droplets also enter a stable state at the end of  $t=1.6$  seconds, their final aggregation morphology differs from the situation considering thermal capillary calculations.

Next, observe the velocity vector distribution of the dual droplets during microchannel polymerization as shown in Figure 8. After the initial stage, droplet A moves with the fluid flow in the microchannel and gradually approaches droplet B. When the time point is  $t=0.68s$  in Figure (a), droplets A and B meet and begin to aggregate. At this time, due to surface stress, small-scale vortex structures are generated in the upper parts of droplets A and B. Subsequently, at the time node  $t=1.6s$  in Figure (b), the aggregated droplet morphology can be seen. It is worth noting that under the influence of thermal capillary convection, a stable internal flow field is formed inside the droplet, with vortex like flow trends on both sides. Although there are some numerical oscillations and instability phenomena in the velocity vector distribution map, the overall numerical calculation is still reliable.

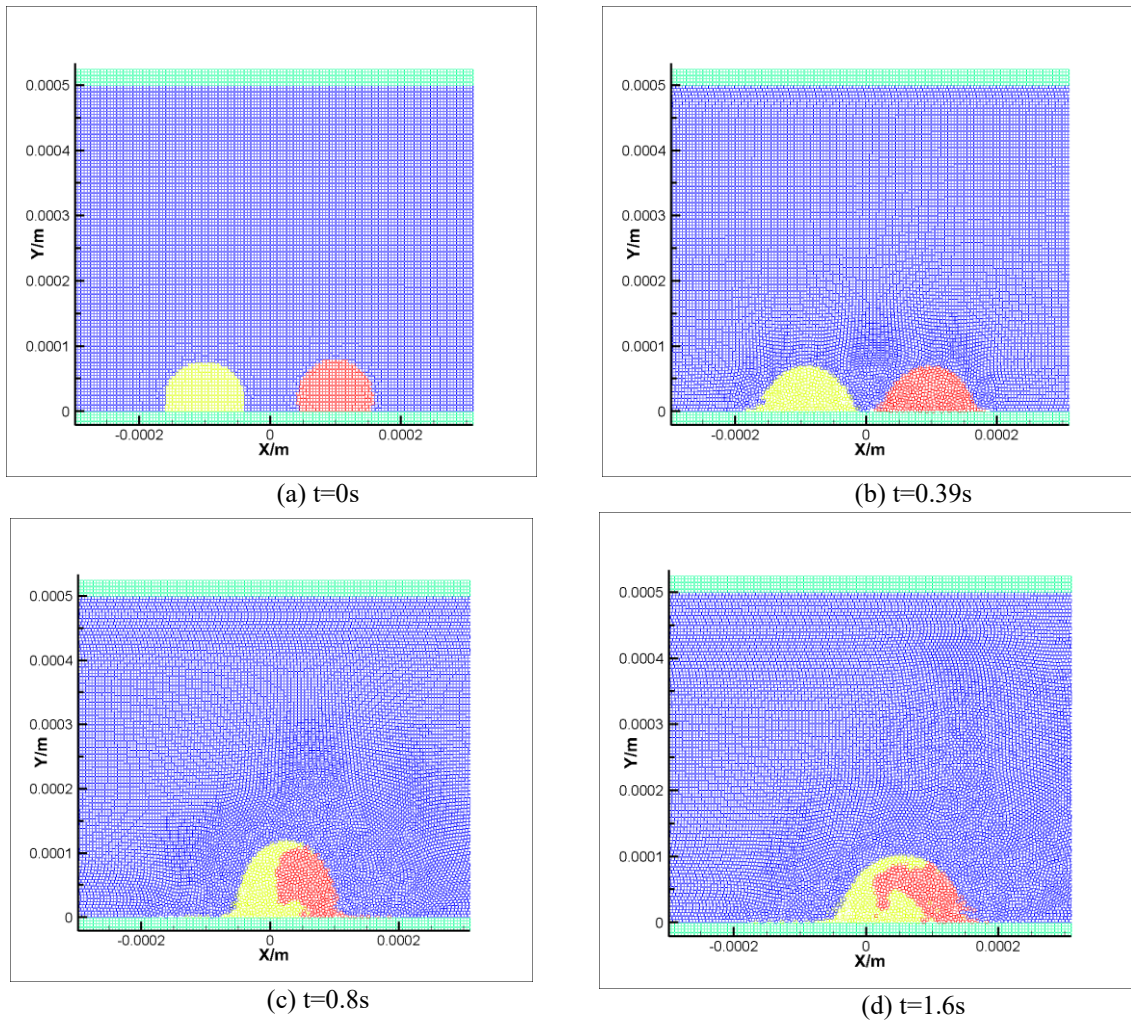


Figure 7: Double Droplet Microchannel Polymerization Problem without Considering Thermal Capillarity Calculation

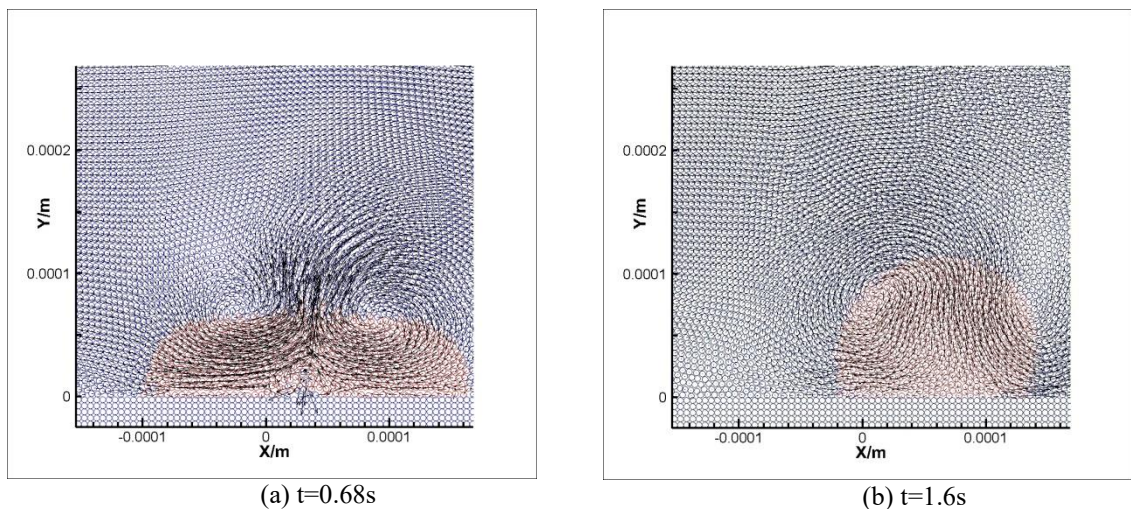


Figure 8: The Velocity Vector Distribution of the Double Droplet Microchannel Polymerization Problem

When exploring the velocity vector distribution of dual droplets in microchannel aggregation scenarios, we delved into the fundamental driving force of fluid thermal capillary convection - the changes in key physical properties such as internal viscosity and thermal conductivity energy of droplets caused by temperature changes, which directly affect the mechanical environment inside and around the fluid. The core manifestation of the viscous properties of droplets is their surface tension, especially in simulating and calculating droplet shape changes, where the normal calculation of surface tension plays an indispensable role.



- [7] Wang Z , Sugiyama T .On the free surface boundary of moving particle semi-implicit method for thermocapillary flow. *Engineering Analysis with Boundary Elements*, 2022, 135:266-283.
- [8] L.B. Lucy, A numerical approach to the testing of the fission hypothesis, *Astron. J.* 82 (1977) 1013–1024.
- [9] R.A. Gingold, J.J. Monaghan, Smoothed particle hydrodynamics: theory and application to non-spherical stars, *Mon. Not. R. Astron. Soc.* 181 (3) (1977)375–389
- [10] Liu SS, He XW, Wang WC, Wu EH. Survey on Fluid Simulation Using Smoothed Particle Hydrodynamics. *Journal of Software*, 2024, 35(1): 481–512
- [11] Peng C, Wang S, Wu W, et.al. LOQUAT: An Open-Source GPU-Accelerated SPH Solver for Geotechnical Modeling. *Acta Geotechnica*. 2019, 14(5): 1269-1287
- [12] Cho H K .Memory-efficient flow accumulation using a look-around approach and its OpenMP parallelization. *Environmental Modelling & Software*, 2023.
- [13] Monaghan J J. Smoothed particle hydrodynamics. *Progress in Physics*, 2005.
- [14] Monaghan J J. Simulating Free Surface Flows with SPH. *Journal of Computational Physics*, 1994, 110(2): 399-406.
- [15] Qiang H F, Gao W R.A new SPH equation including variable smoothing lengths aspects and its implementation. *ISCM*, 2007, Beijing.
- [16] Monaghan J J. SPH without a Tensile Instability. *Journal of Computational Physics*, 2000, 159(2): 290-311.
- [17] Liu H, Qiang H F, Chen F Z. A novel smooth particle dynamics model for solid - wall boundary application, *Acta Physica Sinica*, 2015,64(9):094701.
- [18] Liu G R, Liu M B. Smoothed Particle Hydrodynamics: A meshfree particle method. *Hunan University Press*, 2005.
- [19] Brackbill J U, Kothe D B, Zemach C. A continuum method for modeling surface tension. *Journal of Computational Physics*, 1992, 100: 335-354.
- [20] Morris J P, Fox P J, Zhu Y. Modeling low reynolds number incompressible flows using SPH. *Journal of Computational Physics*, 1997, 136(1): 214-226.
- [21] Zhu Y , Zhang C , Hu X .A dynamic relaxation method with operator splitting and random-choice strategy for SPH. *Journal of Computational Physics*, 2022:458.
- [22] Waqas M , Nasir M , Khan M I ,et al.Marangoni forced convective thermally developed two-phase dusty flow of fluid with heat source/ sink phenomenon. *International Journal of Modern Physics B*, 2023.